Journal of Renewable Materials

Tech Science Press

Study on Thermal Insulation Performance of Cross-Laminated Bamboo Wall

Qingfang Lv[1,*], Weiyang Wang[1] and Ye Liu[1]

[1]Key Laboratory of Concrete and Prestressed Concrete Structures of the Ministry of Education, Southeast University, Nanjing, 210096, China.

[*]Corresponding Author: Qingfang Lv. Email: qingfang_lv@126.com.

Abstract: In recent years, bamboo, as a green building material, has attracted more and more attention worldwide. Inspired by the investigation of cross-laminated timber in structural systems, a new engineered cross-laminated bamboo (CLB) consisting of the cross lamination of bamboo scrimber plates is proposed in this paper. To evaluate its potential in structural applications, the thermal insulation performances of the CLB walls and CLB walls with the EPS foam plate were studied and evaluated by the temperature-controlled box-heat flow meter method. Test results indicated that the thermal insulation performance improved with the increase of thickness, but different wall configurations had little effect on the thermal insulation performance under the same thickness of the CLB wall. The thermal insulation performance of EPS-CLB composite wall was much better than that of CLB wall. In addition, a relatively acceptable accuracy of the theoretical calculations was proved. Finally, the influence of different locations of the EPS foam plate on heat transfer coefficient can be neglected as it was studied based on the validated numerical models.

Keywords: Cross-laminated bamboo; steady-state heat transfer; guarded hot plate method; temperature-controlled box-heat flow meter method; thermal insulation performance

1 Introduction

Bamboo is one of important forest resources, which has more than 75 genera and 1250 species [1]. The total area of bamboo forests has reached 22 million hm^2, mainly distributed in tropical, temperate and even cold zones [2]. Bamboo is a renewable resource with many advantages, such as high strength, fast growth and high yield and the use of the bamboo as construction material is beneficial to the protection of the environment [3]. The raw bamboo is used as basic components in the traditional bamboo buildings. However, due to the variability in geometric size and mechanical properties [4], the raw bamboo cannot meet requirements of physical and mechanical properties specified in modern buildings.

The modern engineered bamboo provides an effective way to solve the above problems and broadens the application of bamboo in structures. There are many kinds of modern engineered bamboo according to its raw material, processing technology and combination mode. The raw materials are mainly divided into five categories according to their geometric dimensions: bamboo chip, bamboo mat, bamboo curtain, bamboo split and bamboo filament [5]. The combination modes can also be divided into two kinds: One is that all raw materials are combined along the direction of the fibers and the other is that all raw materials are not combined along the direction of the fibers. At present, the two most commonly used engineered bamboos are laminated bamboo lumber and bamboo scrimber [3]. Many scholars in China and other countries that has bamboo resources have carried out researches on various aspects of laminated bamboo lumber, such as mechanical properties [6-9], material modification [10,11] and flame retardant properties [12].

However, the laminated bamboo lumber has a limitation that requires bamboo with large diameter as raw material. The bamboo scrimber is made of one-way bamboo filaments by dipping in the glue and

hot-pressing, which has no requirements for raw material [13]. Guan et al. [14] compared bending resistance of timber scrimber and bamboo scrimber through experiments, which indicated that the longitudinal flexural modulus of elasticity of bamboo scrimber is better than that of timber scrimber when their densities are larger than 0.7 g/cm^3 and the longitudinal flexural strength of bamboo scrimber is better than that of timber scrimber when their densities are larger than 0.8 g/cm^3. Many scholars have studied different aspects of bamboo scrimber, such as mechanical properties [15-17], flame retardant properties [18,19] and material modification [20,21].

There have been many studies on mechanical properties of bamboo and bamboo components, but there are relatively few studies on thermal insulation performance of engineering bamboo composites [22,23], especially on the thermal insulation performance of bamboo scrimber as wall material. Gao et al. [24] prepared three kinds of bamboo-wood composite wall, among which bamboo curtain plywood was used for bamboo board, and evaluated their thermal insulation and sound insulation performance, revealing the influence of wall materials and internal filling materials on the thermal insulation and sound insulation performance of the wall. Wang et al. [25] carried out experiments on four different configurations of composite shear walls, including one classical full wood-based configuration, one hybrid bamboo-wood-based configuration and two full bamboo-based configurations with different studs thickness, to study their thermal insulation performance. The results showed that the thermal insulation performances of engineered bamboo composites are slightly lower compared with wood composites and there is the possibility of using bamboo-based shear walls in light-frame buildings ensuring thermal insulation performances similar to classical wood-based one.

The above bamboo composite walls are all used in the light frame construction. In order to break through the height limitation of light bamboo structure and promote the development of modern heavy bamboo structure, a new engineering cross-laminated bamboo (CLB) is proposed in this study inspired by cross-laminated timber (CLT). So as to explore the application feasibility of walls made of CLB, a series of experiments were carried out to investigate the thermal insulation performance of CLB walls and CLB walls with the EPS foam plate (EPS-CLB composite walls). The objectives of this study are: (1) to study the effect of different wall thickness and different wall configurations on heat transfer of CLB walls and EPS-CLB composite walls; (2) to establish validated numerical models for the deeper research on the effect of different EPS locations on the heat transfer in the wall.

2 Heat Transfer Analysis of CLB Wall and EPS-CLB Composite Wall

In this section, the thermal conductivity coefficient λ of bamboo scrimber plate and EPS foam plate and the heat transfer coefficient K of CLB wall and EPS-CLB composite wall were measured through experiments. According to the experimental results, the thermal insulation performance of 5 CLB walls and 5 EPS-CLB composite walls were analyzed. In addition, the theoretical values of K of walls calculated from λ of bamboo scrimber plate and EPS foam plate were compared with the experimental values of K of walls measured by experiments.

2.1 Thermal Conductivity Coefficient Test

2.1.1 Test Specimens and Methodology

Thermal conductivity coefficients of two types of plates are measured in this paper, including the bamboo scrimber plate and EPS foam plate. The raw material of the bamboo scrimber is selected from the moso bamboo in the Huangshan area of Anhui Province, China. Bamboo scrimber plates are made by Anhui Bamboo Track New Material Science and Technology Co., Ltd. The specific production process is as follows: (1) Firstly, the bamboo is soaked in the hot alkaline solution to be softened; (2) Secondly, the softened bamboo is processed into bamboo filaments through roller press and then dried; (3) Thirdly, the bamboo filaments are soaked with glue and then dried again; (4)Finally, the dried bamboo filaments dipped in glue are placed uniformly and directionally, and then hot-pressed to the bamboo scrimber plate.

The bamboo scrimber plate has an average bulk density of 1200 kg/m^3 and the moisture content of bamboo scrimber plate is about 7% in this test. The 30 mm thick peeled high density EPS foam plates, used as the thermal insulation plate, are produced by Yiwu Zeke Packaging Factory in Jinhua city, Zhejiang province, China. The average bulk density of the EPS foam plate is 25 kg/m^3, only about 2.08% of the bamboo scrimber plate. The adhesive is 1-K-PUR adhesive produced by Jowat Adhesive Co., Ltd. in Beijing, China. The specific heat capacity of the adhesive is 1150 J/(kg·K) and the thermal conductivity coefficient of the adhesive is about 0.3 to 0.6 W/(m·K), which is provided by the manufacturer.

Three groups of bamboo scrimber plate specimens A1-A3 were used to determine the thermal conductivity coefficient of the bamboo scrimber plate and three groups of bamboo scrimber plates specimens B1-B3 were used to study the effect of the average temperature on the thermal conductivity. Three groups of EPS foam plate specimens C1-C3 were used to determine the thermal conductivity coefficient of the EPS foam plate. Each group has two specimens and all the above specimens are 300 mm × 300 mm × 30 mm ($l \times b \times d$) in dimension. In order to improve the accuracy of the test results, the surface of all tested specimens should be machined as flat as possible in the manufacturing process to ensure the good contact between the tested specimens and test apparatus.

The method of determining steady-state thermal conductivity properties of the bamboo scrimber and EPS foam plates by the guarded hot plate apparatus was carried out according to the provision of ISO 8302: 1991 [26]. A DRH-300 thermal conductivity apparatus (a Double-sides Guarded Hot Plate apparatus) is shown in Fig. 1, which can test one group of two specimens at the same time. This apparatus can test materials with thermal conductivity coefficients from 0.01 W/(m·K) to 2 W/(m·K) and its test error can be controlled within 3%.

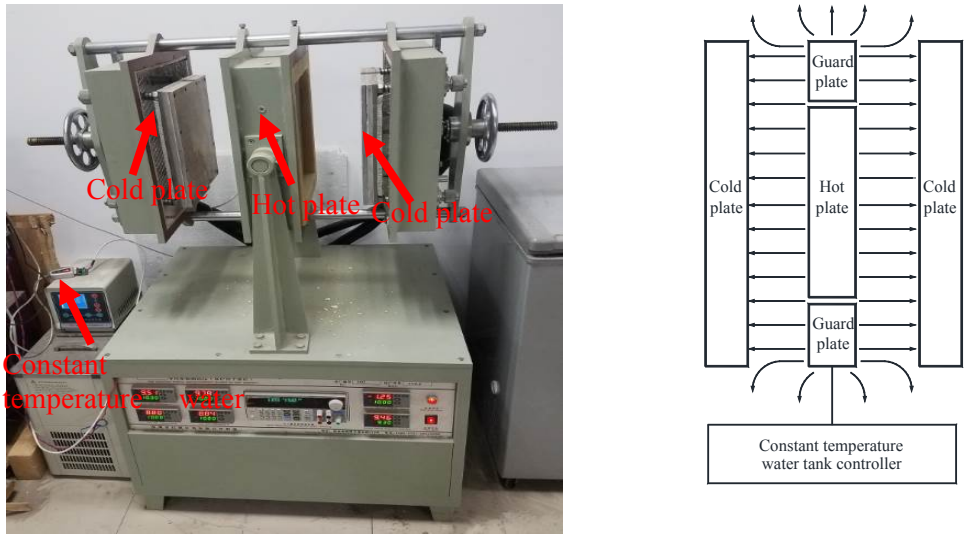

Figure 1: Test apparatus for measuring the thermal conductivity coefficient

The thermal conductivity coefficient λ can be evaluated according to ISO 8302:1991 [26] as follows:

$$\lambda = \frac{\Phi \cdot d}{A\left(T_1 - T_2\right)} = \frac{I \cdot U \cdot d}{A \cdot \Delta T} = \frac{q \cdot d}{\Delta T} \tag{1}$$

where Φ is the power of the heating plate, W; d is the average thickness of each group, m; A is measurement area, m^2. In the present test apparatus, it is calculated as twice the surface area of each tested specimen and thus recognized as $2lb$; T_1, T_2 are the average value of the hot and cold surface of the test pieces, respectively, °C; I is the current passing through the heating plate, A; U is the voltage of the heating plate, V.

2.1.2 Test Results and Discussions about λ

Test results and calculation results based on Eq. (1) for bamboo scrimber and EPS foam plates are listed in Tab. 1 and Tab. 2, respectively.

Table 1: Test results of bamboo scrimber plates

Group	T_2/℃	T_1/℃	T_{ave}/℃	I/A	U/V	λ_B/(W/(m·K))
A1	10.19	30.13	20.16	0.616	13.27	0.264
A2	10.25	30.18	20.22	0.614	13.26	0.259
A3	10.07	30.09	20.08	0.617	13.31	0.265
B1	10.11	20.01	15.06	0.439	9.12	0.260
B2	10.25	40.28	25.26	0.741	16.55	0.268
B3	10.32	50.39	30.36	0.826	19.12	0.273

Note: T_{ave} is the average value of temperatures at cold and hot plates; λ_B is the thermal conductivity coefficient of the bamboo scrimber plate.

Table 2: Test results of EPS foam plates

Group	T_2/℃	T_1/℃	T_{ave}/℃	I/A	U/V	λ_E/(W/(m·K))
C1	10.02	30.10	20.06	0.236	5.089	0.040
C2	10.15	30.21	20.18	0.237	5.108	0.042
C3	10.11	30.08	20.10	0.235	5.063	0.039

Note: λ_E is the thermal conductivity coefficient of the EPS foam plate.

According to the test results of the above tables, the average values of the thermal conductivity coefficients of the bamboo scrimber plate λ_B obtained from groups A1-A3 and EPS foam plate λ_E obtained from groups C1-C3 are 0.263 W/(m·K) and 0.040 W/(m·K), respectively. As observed from groups B1-B3 in Tab. 1, the value of λ_B only slightly increases with the average temperature. λ_B increases from 0.260 W/(m·K) in the group B1 to 0.273 W/(m·K) in the group B3 with the increase of T_{ave} from 15.06°C to 30.36°C, and the increase of λ_B is only 5.0%. Therefore, the influence of the average temperature on the thermal conductivity coefficient of the bamboo scrimber plate can be neglected in the thermal calculation. The slight increase of the thermal conductivity coefficient with the increase of the average temperature can be explained as follows: As the average temperature increases, the thermal motion of the bamboo solid molecules and free water molecules in bamboo increases. The thermal conductivity of the air in the pores and radiation heat transfer between the pore walls are also enhanced. Therefore, the combined action of gas phase and solid phase makes the thermal conductivity of bamboo slightly increase with the increase of the average temperature.

Thermal conductivity coefficients of commonly used building materials are listed in Tab. 3 per Chinese standard GB50176-2016 [27]. Compared with most existing common inorganic materials used in building, the thermal conductivity coefficient of the bamboo scrimber plate is far less than that of these materials, which is about 15% of reinforced concrete and about 50% of hollow brick and light-weight aggregate concrete. The EPS foam plate has the superb thermal insulation performance and λ_E is only 0.04 W/(m·K), which is about 15.2% of λ_B. Although the EPS foam plate has excellent thermal insulation performance, the compressive capacity of the EPS foam plate is poor, which makes it cannot be independently used to satisfy requirements of load bearing. The mechanical properties of bamboo scrimber plate are good [3]; and therefore, the bamboo scrimber plate and EPS foam plate can be combined to achieve a good thermal insulation effect and satisfy bearing capacity requirements.

Table 3: Thermal conductivity coefficients of commonly used building materials [27]

Material	λ/(W/(m·K))	Material	λ/(W/(m·K))
Reinforced concrete	1.74	Pine, timber, spruce (parallel to grain)	0.29
Light weight aggregate concrete	0.42-1.00	Pine, timber, spruce (transverse to grain)	0.14
Cement mortar	0.93	Building sand	0.58
Clay brick masonry	0.76-0.81	Granite, basalt	3.49
Autoclaved fly ash-lime brick	0.74	Glass	0.52-0.76
Hollow brick masonry	0.44-0.58		

2.2 Heat Transfer Analysis of CLB Wall and EPS-CLB Composite Wall

2.2.1 Test Specimens

CLB is formed by the cross lamination of bamboo scrimber plates introduced in Section 2.1.1. The adhesives used in CLB walls and EPS-CLB composite walls is 1-K-PUR adhesive produced by Beijing Youward Adhesive Co., Ltd, China. According to Chinese climate and energy-saving design requirements [28-31], the thicknesses of walls are determined to be 90 mm, 120 mm, 150 mm, 180 mm and 210 mm, respectively, considering the bearing requirements. In order to investigate the effect of different wall thicknesses and different wall configurations on heat transfer, 5 CLB walls and 5 EPS-CLB composite walls were designed in this test. Each specimen has the same length and width of 980 mm and the thicknesses of all tested wall specimens are listed in Tab. 4. Detailed configurations of the tested wall specimens are shown in Fig. 2. The thicknesses of EPS foam plates are all 30 mm.

Table 4: Specific thicknesses of different walls

Label	B3(30)E0	B4(30)E0	B6(20)E0	B3(40)E0	B5(30)E0
Thickness/mm	88	121	120	120	145
Label	B3(30)E1	B3(40)E1	B3(40)E2	B5(30)E1	B5(30)E2
Thickness/mm	117	149	178	175	204

Note: B3 means three layers of bamboo scrimber plates. (30) means that the thickness of the bamboo scrimber plate is 30 mm. E0 means no EPS foam plate. Therefore, B3(30)E0 means the specimen composed with three 30 mm bamboo scrimber plates and no EPS foam plate.

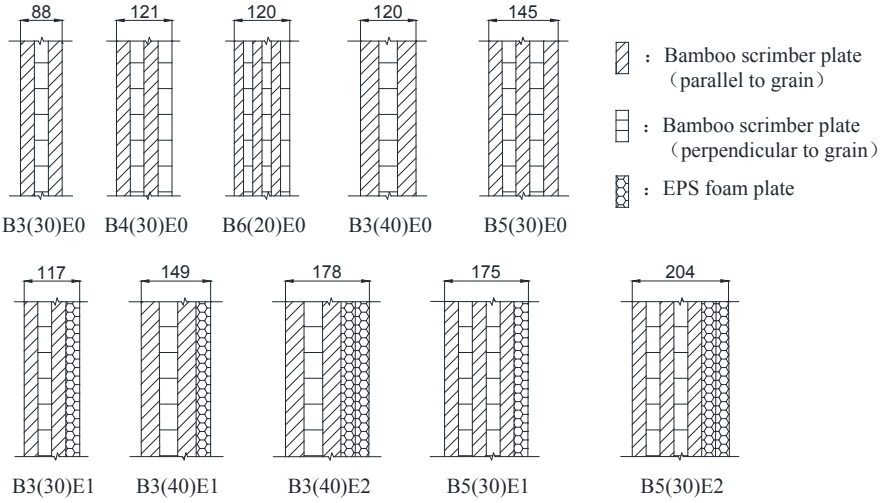

Figure 2: Detailed configurations of specimens

2.2.2 Test Protocol

The temperature controlled box-heat flow meter method [32] which combines heat flow meter method and hot box method is used in the present study. The instrument selected for this test is JTRG-1 type heat transfer performance detection device produced by Beijing Century Jiantong Technology Co., Ltd., China, as shown in Fig. 3. Specific technical indicators of JTRG-1 type detection apparatus are summarized as follows: (1) Parameters of the hot box. Temperature control range: 15°C to 50°C, temperature control accuracy: ± 0.2°C; (2) Parameters of the cold box. Temperature control range: -10°C to 20°C; (3) Specimen specification: 1000 mm × 1000 mm × 400 mm.

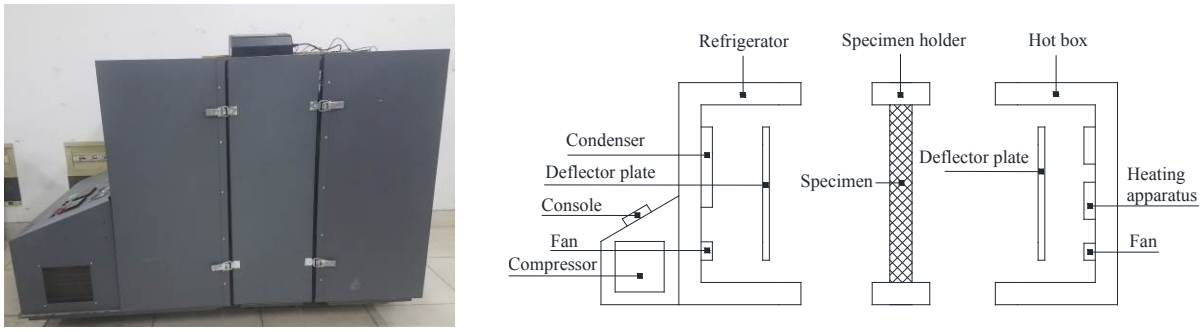

Figure 3: Test apparatus for heat transfer coefficient

The specific operation process is summarized as follows: (1) Installation of test specimens. The CLB wall is installed in the test holder, and the polyurethane foaming agent is used to fill the voids around the specimens to ensure good sealing so as to prevent air convection in the cold and hot boxes. (2) Layout measuring points. Three heat flow measuring points (recorded as HF1, HF2 and HF3, respectively) and six temperature measuring points (recorded as HT1 to HT6, respectively) are evenly arranged on the hot side of the walls, and the temperature measuring points are close to the heat flow measuring points. Six temperature measuring points (recorded as CT1 to CT6, respectively) are arranged on the cold side of the wall, as shown in Fig. 4. (3) Set of temperature. The temperatures of cold and hot boxes are set as -5°C and 26°C, respectively. (4) Data acquisition. All data are automatically collected every 15 minutes.

(a) Hot side (b) Cold side

Figure 4: Layout of sensors on the wall

The heat transfer coefficient K within one measurement cycle can be calculated based on Eq. (2) per ISO 8990:1994(E) [33] and Chinese standard JGJ/T132-2009 [34]. The average value of the heat transfer coefficient with an error less than 1% between two consecutive measurement cycles is taken as the acceptable test result.

$$K = \frac{1}{R'} = \frac{1}{R_i + R + R_e} \tag{2}$$

where R' is the total heat transfer resistance, (m^2·K)/W; R_i and R_e are internal and external surface heat transfer resistances of the wall, respectively. According to Chinese standard 'Code for thermal design of civil building GB50176-2016' [27], R_i, R_e are respectively taken as 0.11 (m^2·K)/W and 0.04 (m^2·K)/W in this study; R is the heat transfer resistance of the wall, (m^2·K)/W. The thermal resistance R can be calculated as follows:

$$R = \frac{\sum_{j=1}^{n}\left(\theta_{1j} - \theta_{2j}\right)}{\sum_{j=1}^{n} q_j} \tag{3}$$

where θ_{1j}, θ_{2j} are the jth measurement cycle of the inside and outside surface temperature of the wall, respectively, ℃; q_j is the jth measurement cycle of the heat flow density of the wall, W/m^2.

2.3 Test Results and Discussions

2.3.1 Description of Test Results

The test results are shown in Fig. 5. The value of CT_{ave} is the average value of CT1 to CT6. The value of HT_{ave} is the average value of HT1 to HT6. The value of HF_{ave} is the average value of HF1 to HF3.

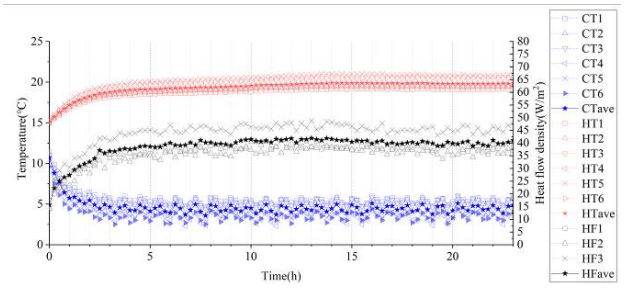

(a) B3(30)E0

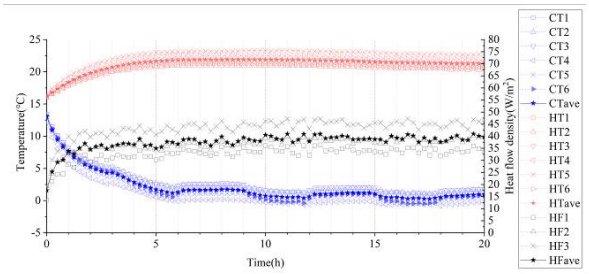

(b) B4(30)E0

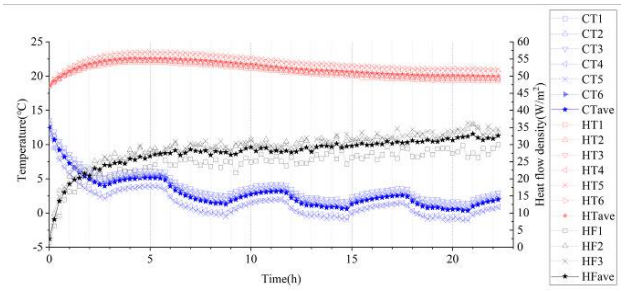

(c) B6(20)E0

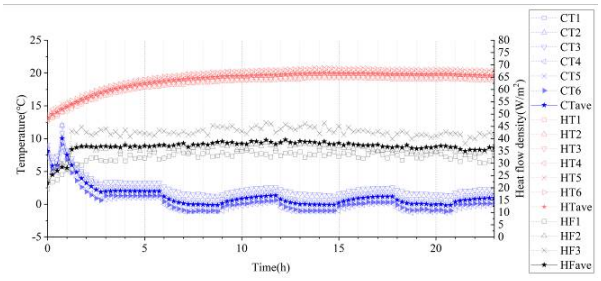

(d) B3(40)E0

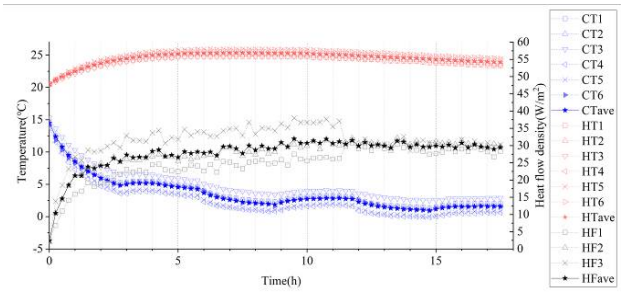

(e) B5(30)E0

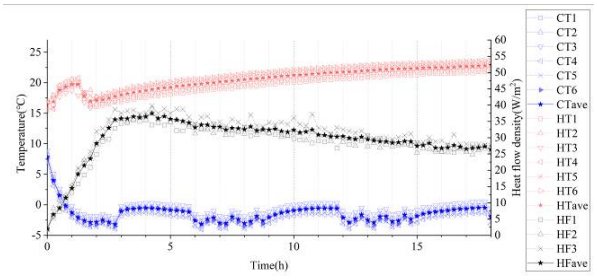

(f) B3(30)E1

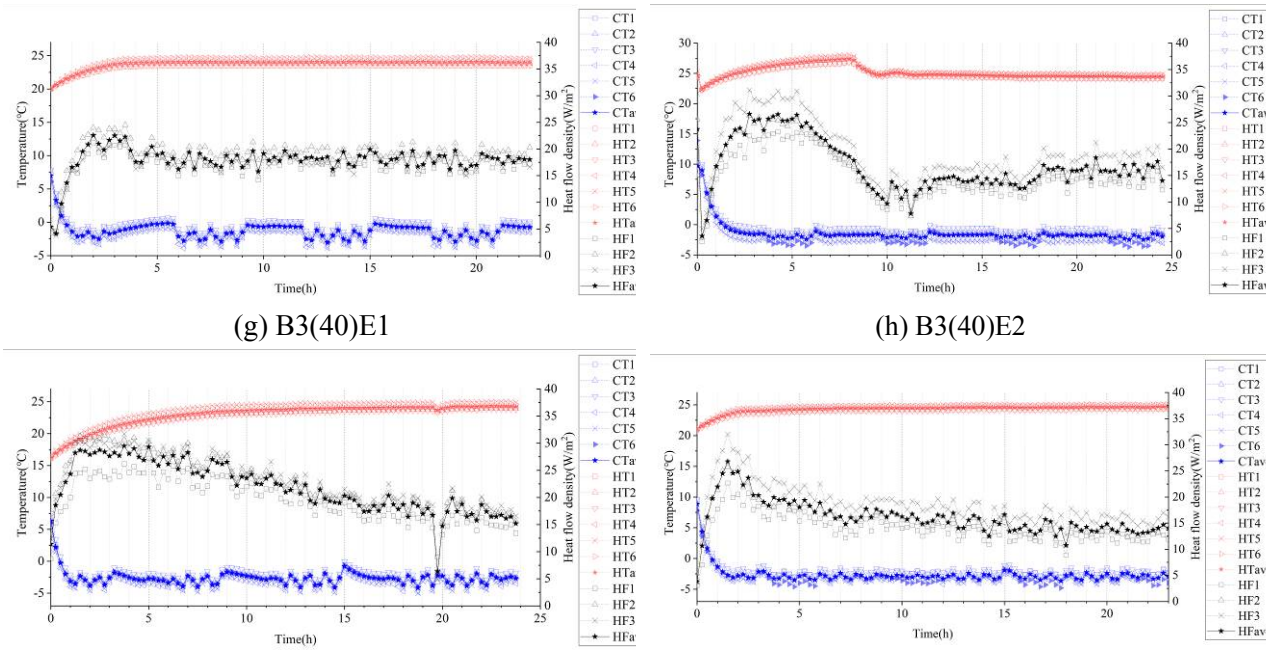

(g) B3(40)E1 (h) B3(40)E2

(i) B5(30)E1 (j) B5(30)E2

Figure 5: Distributions of the heat flow and temperature over time

The average value of the heat flow densities (HF_{ave}) of different walls are compared, which is shown in Fig. 6. As can be seen from the Figs. 6(a), 6(b) and 6(c), the HF_{ave} of the wall with one EPS foam plate is about 37% to 51% lower than that of the same wall with no EPS foam plate. However, the HF_{ave} of the wall with two-layer EPS foam plates is comparable to the same wall with one-layer EPS foam plate, reducing less than 16%. The comparison of the HF_{ave} of different walls with the similar thickness is shown in the Fig. 6(d), which shows that the HF_{ave} of B3(30)E1 is the lowest and HF_{ave} is affected by the different configuration of the wall. In the condition of the same thickness of the bamboo scrimber plates, the HF_{ave} of B6(20)E0 is the lowest and the HFave of B3(40)E0 and B4(30)E0 are similar, which can be explained that when heat flow passes through cross layers, obstacles will appear to reduce the heat flow density.

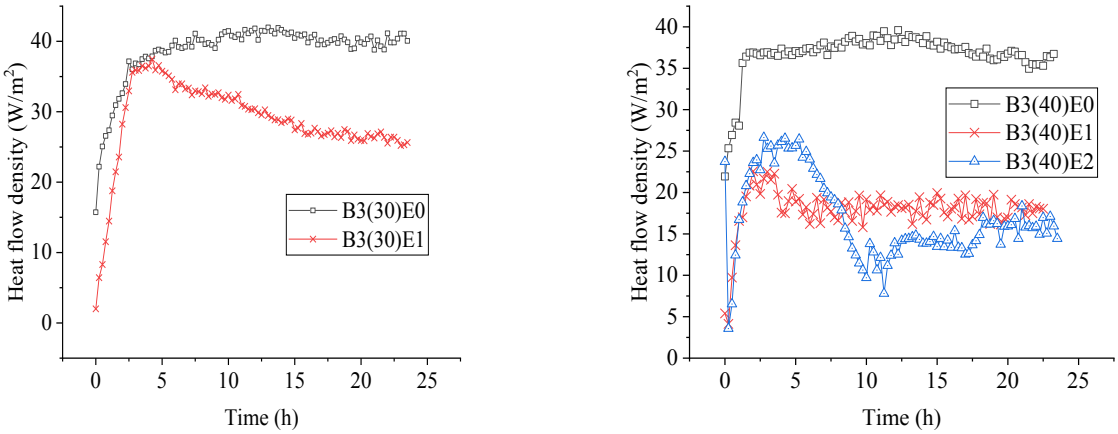

(a) (b)

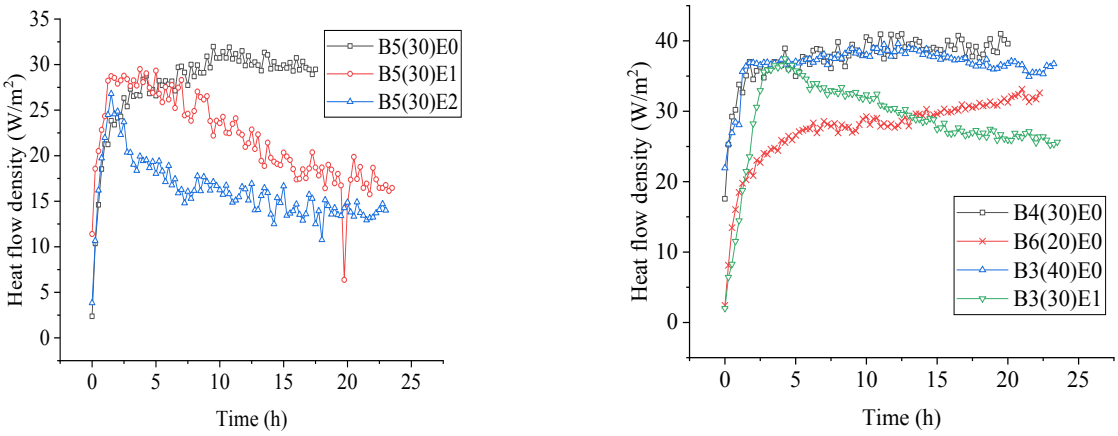

(c) (d)

Figure 6: Comparison of the heat flow density

2.3.2 Analysis of Heat Transfer Coefficient

Based on the measured values and Eqs. (2), (3), the heat transfer coefficient in a single measurement cycle (generally 3 hours) is calculated. The average value K_{ave} of two consecutive cycles with an error less than 1% is adopted, as listed in Tab. 5.

Table 5: Calculation results of heat transfer coefficients

Label	R_1/((m²·K)/W)	K_1/(W/(m²·K))	R_2/((m²·K)/W)	K_2/(W/(m²·K))	$\lvert K_1-K_2\rvert/K_2$	K_{ave}/(W/(m²·K))
B3(30)E0	0.384	1.874	0.386	1.867	0.37%	1.871
B4(30)E0	0.528	1.470	0.533	1.464	0.41%	1.467
B6(20)E0	0.597	1.336	0.601	1.332	0.30%	1.334
B3(40)E0	0.531	1.468	0.534	1.466	0.14%	1.467
B5(30)E0	0.762	1.094	0.764	1.098	0.21%	1.096
B3(30)E1	0.951	0.913	0.945	0.914	0.11%	0.914
B3(40)E1	1.412	0.637	1.444	0.635	0.31%	0.636
B3(40)E2	1.674	0.553	1.650	0.552	0.18%	0.552
B5(30)E1	1.620	0.569	1.761	0.564	0.89%	0.567
B5(30)E2	2.007	0.468	2.011	0.471	0.85%	0.470

Note: K_1 and R_1 are the heat transfer coefficient and thermal resistance calculated from the data in the last measurement cycle, respectively. K_2 and R_2 are the heat transfer coefficient and thermal resistance calculated from the data in the second to last measurement cycle, respectively.

According to Chinese standard [28-31], CLB walls with thickness over 120 mm can meet the energy-saving design requirements in Hot summer and warm winter zone. EPS-CLB composite walls can meet the energy-saving design requirements in Moderate climate (A) zone and Hot summer and cold winter zone. The specimen B5(30)E2 whose K is 0.470 W/(m²·K) can even meet the energy-saving design requirements in Cold zone, showing excellent thermal performance.

(1) Effect of different thicknesses and configurations on heat transfer coefficients of CLB walls

Heat transfer coefficients of CLB walls specimens without EPS foam plate are shown as Fig. 7. It is found that the heat transfer coefficient of the CLB wall decreases with the increase of the wall thickness. When the wall thickness increases from 88 mm in specimen B3(30)E0 to 145 mm in specimen B5(30)E0, the heat transfer coefficient decreases from 1.871 W/(m²·K) to 1.096 W/(m²·K). Even in specimen B5(30)E0, the heat transfer coefficient is still relatively high and larger than 1.0 W/(m²·K). According to Eq. (2), the thermal

resistance R is inversely proportional to heat transfer coefficient K. With the increase of the wall thickness, R increases linearly and K decreases at a lower rate. It is uneconomical and impractical to realize the requirements of energy-saving design only depending on thickening the CLB wall.

The heat transfer coefficients of specimens B4(30)E0, B6(20)E0 and B3(40)E0 are similar and the maximum difference of the heat transfer coefficient between specimens B6(20)E0 and B3(40)E0 is 9.07%. The configuration has only little effect on the heat transfer performance. Therefore, the influence of configuration on heat transfer performance can be neglected.

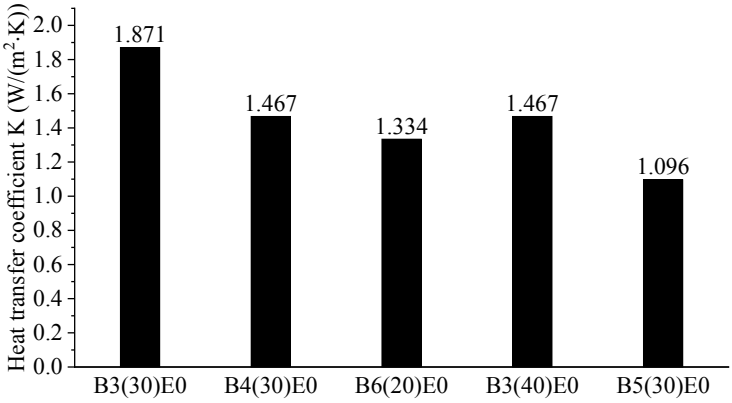

Figure 7: Heat transfer coefficients of CLB walls

(2) Effect of EPS foam plate on heat transfer coefficient of CLB wall

According to the heat transfer test of walls, the comparison of heat transfer coefficients of CLB walls and EPS-CLB composite walls is shown in Fig. 8. In general, the heat transfer coefficients of CLB walls are much larger than EPS-CLB composite walls. After adding one layer of 30-mm EPS foam plate to the external surface of the CLB wall, the heat transfer coefficient of the CLB wall decreases significantly. Compared with the specimen B3(30)E0 composed of three 30-mm bamboo scrimber plates, the heat transfer coefficient of specimen B3(30)E1 composed of three 30-mm bamboo scrimber plates and one 30-mm EPS foam plate decreases by 51.1%. Compared with the specimen B3(40)E0, the heat transfer coefficient of the B3(40)E1 specimen is reduced by 56.6%. Compared with the specimen B5(30)E0, the heat transfer coefficient of the specimen B5(30)E1 is reduced by 48.3%. Therefore, the use of the external thermal insulation has an important effect on the heat transfer performance of the CLB wall.

The heat transfer coefficient of specimen B3(40)E2 with two layers of 30-mm EPS foam plate decreases by 13.2% compared with the specimen B3(40)E1 which contains one layer of the EPS foam plate. Compared with specimen B5(30)E1, the heat transfer coefficient of specimen B5(30)E2 decreases by 17.1%. Compared with the efficiency of adding one layer of the thermal insulation plate to improve the thermal insulation effect, the efficiency of adding two layers of thermal insulation plates is obviously reduced. The contribution of the EPS thermal insulation plate to the reduction of heat transfer coefficient is becoming small with the increasing layers of EPS foam plates because the magnitude of the thermal resistance R is inversely proportional to heat transfer coefficient K rather than being linear.

The heat transfer coefficient of B3(40)E2 with a thickness of 178 mm is only 2.6% lower than that of B5(30)E1 with a thickness of 175 mm. The total thickness of specimens B3(40)E2 and B5(30)E1 is almost the same, but the load bearing of the specimen B5(30)E1 is obviously larger than that of the specimen B3(40)E2 because the total thickness of bamboo scrimber plates in B5(30)E1 is about 30 mm larger than that in B3(40)E2. Therefore, under the condition of same thickness, the configuration of specimen B5(30)E1 is more reasonable than that of specimen B3(40)E2. The thermal insulation capacity and load-bearing capacity should be considered simultaneously in the design of CLB wall.

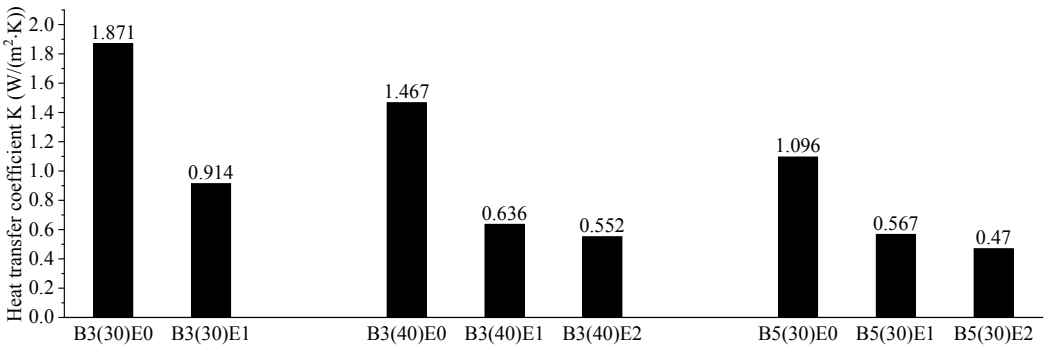

Figure 8: Heat transfer coefficients of specimens whether contain thermal insulation

2.3.3 Comparison of Theoretical and Experimental Values of Heat Transfer Coefficient

According to the thermal resistance calculation method of the wall composed of homogeneous material layers in ISO 6946:1996 [35], the thermal resistance of each layer is calculated to obtain the thermal resistance of the wall. The equation is proposed as follows:

$$R = R_B + R_{\mathrm{E}} = \frac{\delta_{\mathrm{B}}}{\lambda_{\mathrm{B}}} + \frac{\delta_{\mathrm{E}}}{\lambda_{\mathrm{E}}} \tag{4}$$

where δ_B is the total thickness of the bamboo scrimber plates, m; δ_E is the total thickness of the EPS foam plate, m. The above equation calculates the thermal resistance based on the thickness and thermal conductivity of each ideal homogeneous plate in the wall, while Eq. (3) directly measures the thermal resistance of the wall by testing. The theoretical values of heat transfer coefficient are calculated based on the Eq. (2) and Eq. (4), which are also compared with the experimental values based on the Eq. (2) and Eq. (3). The relevant results are listed in Tab. 6.

Table 6: Comparison between K_t and K_e

Label	R_t/((m²·K)/W)	K_t/(W/(m²·K))	K_e/(W/(m²·K))	($\lvert K_e$-$K_t\rvert/K_e$)
B3(30)E0	0.335	2.064	1.871	10.29%
B4(30)E0	0.460	1.639	1.467	11.73%
B6(20)E0	0.456	1.649	1.334	23.64%
B3(40)E0	0.456	1.649	1.467	12.43%
B5(30)E0	0.551	1.426	1.096	30.10%
B3(30)E1	1.081	0.812	0.914	11.11%
B3(40)E1	1.206	0.737	0.636	15.93%
B3(40)E2	1.949	0.476	0.552	13.68%
B5(30)E1	1.301	0.689	0.567	21.52%
B5(30)E2	2.048	0.455	0.470	3.18%

Note: R_t is theoretical value of the thermal resistance of walls; K_t is theoretical value of the heat transfer coefficient; K_e is experimental value of the heat transfer coefficient.

As listed in Tab. 6, the theoretical heat transfer coefficient is generally larger than the experimental heat transfer coefficient. The reasons for the errors between the experimental and theoretical heat transfer coefficients are summarized as follows:

(1) The actual EPS foam and bamboo scrimber are not completely homogeneous materials.

(2) There are voids between the layers in the wall, which makes the resistance of heat flow is relatively large when passing from one layer to anther adjacent layer.

(3) The water content has an effect on the thermal conductivity. Because the tests in Section 2.1 and Section 2.2 are not conducted at the same time, the water content of the walls in Section 2.2 may be different from that of the specimens in Section 2.1. The theoretical results of the heat transfer coefficient are obtained by the thermal resistance calculated by the thermal conductivity coefficient in Section 2.1. Therefore, there are some deviations between theoretical results and experimental results measured by the controlled box heat flow meter method directly.

3 Finite Element Analysis

In this section, numerical models were established by finite element software ABAQUS to analyze the steady-state heat transfer of the specimens. Firstly, due to the uncertainty of the thermal conductivity coefficient of adhesive λ_A provided by the manufacturer, the effect of different λ_A on the thermal insulation performance of walls was studied. Moreover, numerical simulation results were compared with the representative experimental results, including specimens B3(40)E0 and B5(30)E1, to determine the effectiveness of the established numerical models. Finally, the effect of EPS foam plate location on thermal insulation was explored.

3.1 Steady-state Heat Transfer Analysis

3.1.1 Basic Hypothesis

Because of the complexity of factual situation, some assumptions are adopted in the finite element analysis (FEA) for ease of analyzing the heat transfer of the walls without affecting the correctness. The adopted assumptions are summarized as follows:

(1) The layers of CLB wall and EPS-CLB composite wall (bamboo scrimber plates, adhesive layers and EPS foam plate) are all homogeneous and isotropic materials. The thermophysical parameters of these materials are constant and are not affected by temperature, humidity and pressure, etc.

(2) The interfaces between layers of the wall fully contact with each other and the influence of the interface thermal resistance [36] is not considered.

(3) The atmosphere temperature is assumed as constant.

3.1.2 Establishment of Numerical Model

According to Section 2.2.1, the length and width of the models B3(40)E0 and B5(30)E1 are all 980 mm and the thicknesses of these two models are 120 mm and 204 mm, respectively. The thickness of adhesive layer was taken as 0.1 mm. Based on above test results, the thermal conductivities of bamboo scrimber and EPS foam is 0.263 W/(m·K) and 0.04 W/(m·K), respectively. The specific heat capacities C of bamboo scrimber and EPS foam are 1570 J/(kg·K) and 1380 J/(kg·K) [27,37]. The thermophysical parameters of adhesive are provided by the manufacturer, which are listed in Tab. 7. 8-node linear heat transfer brick elements (DC3D8) were used. Different layers were tied together, which made two materials at the same temperature on the contact surface.

Table 7: Thermophysical parameters of materials in the wall

Material	λ/(W/(m·K))	C/(J/(kg·K))
Bamboo scrimber	0.263	1570
EPS foam	0.04	1380
Adhesive	0.3~0.6	1150

In order to compare with experimental results, the temperatures on both sides of the wall were set to 26°C and -5°C to simulate indoor and outdoor environment, respectively. According to Chinese standard GB50176-2016 [27], the surface heat transfer coefficients of internal and external surface are 8.7 W/(m^2·K)

and 23.0 W/(m^2·K), respectively. The solid surface emissivity ε_r is 0.9 [38] considering surface radiation between atmosphere and both surfaces of the wall. The absolute zero and Stefan-Boltzmann constant [38] were set to -273.15°C and 5.67 × 10-8 W/(m^2·K^4) in the numerical model, respectively. In order to improve the accuracy of heat transfer analysis, the mesh was refined locally in the direction of wall thickness.

3.1.3 Effect of Different Thermal Conductivity of the Adhesive λ_A on the Heat Transfer of Walls

Because of the uncertain range of thermal conductivity of the adhesive listed in Tab. 7, the effect of different values of λ_A on the heat transfer of the tested walls is analyzed in this section. The specimen B6(20)E0 is chosen to be analyzed when λ_A varies from 0.3 W/(m·K) to 0.6 W/(m·K), because the proportion of the total thickness of the adhesive layer to the total thickness of the wall is the largest in all tested walls and the effect caused by the difference of λ_A on the heat transfer of the wall is largest. The temperature distribution contours and heat flow density distribution contours in Z direction of B6(20)E0 are shown in Fig. 9 and Fig. 10.

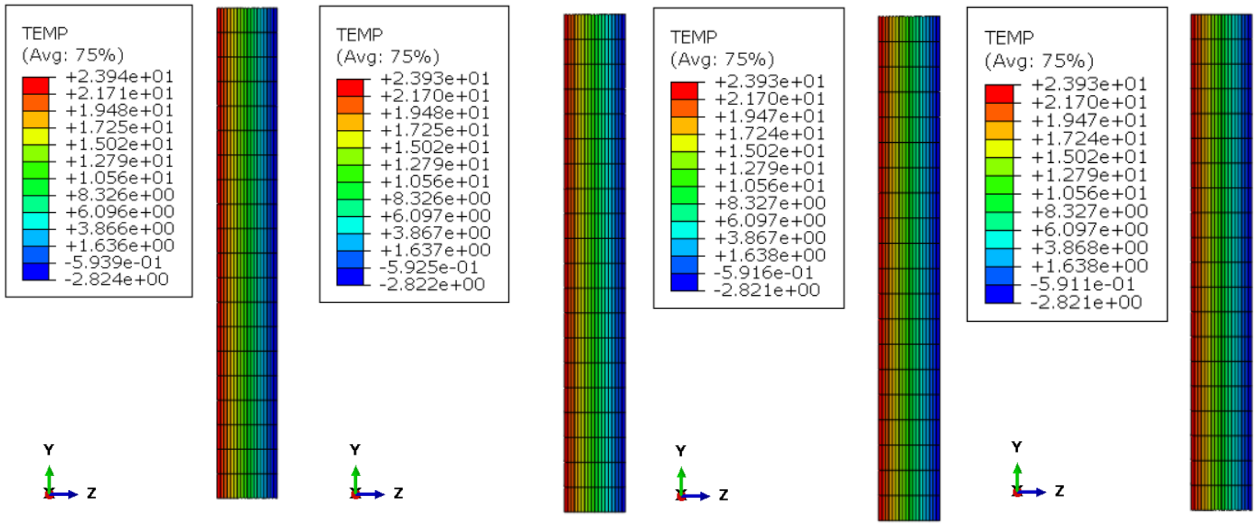

(a) λ_A is 0.3 W/(m·K) (b) λ_A is 0.4 W/(m·K) (c) λ_A is 0.5 W/(m·K) (d) λ_A is 0.6 W/(m·K)

Figure 9: Temperature distribution contours of the model B6(20)E0

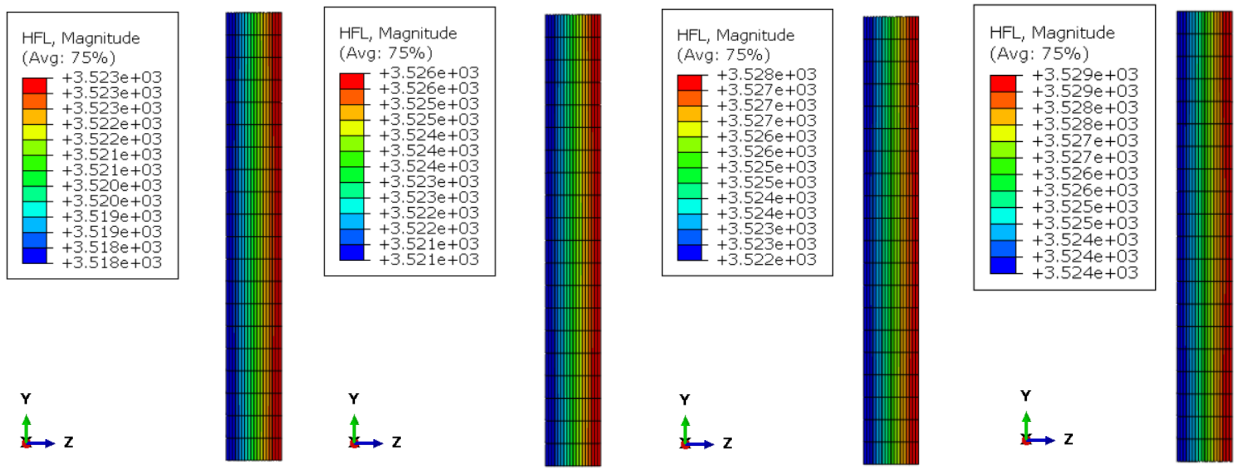

(a) λ_A is 0.3 W/(m·K) (b) λ_A is 0.4 W/(m·K) (c) λ_A is 0.5 W/(m·K) (d) λ_A is 0.6 W/(m·K)

Figure 10: Heat flow density distribution contours of the model B6(20)E0

As can be seen from the above figures, there are few changes observed in the temperature distribution of B6(20)E0 and the heat flow densities on both sides of the model vary monotonously when λ_A increases from 0.3 W/(m·K) to 0.6 W/(m·K). The maximal heat flow density on the hot side of B6(20)E0 increases from 3518 J/(min·m^2) to 3524 J/(min·m^2) when λ_A changes from 0.3 W/(m·K) to 0.6 W/(m·K), increasing by only 0.17%. Based on Eqs. (2) and (3), the thermal resistance R and heat transfer coefficient K can be obtained by the temperature difference ΔT and heat flow densities q on both sides of the model B6(20)E0, as listed in Tab. 8.

Table 8: FEA results of B6(20)E0 in the condition of different values of λ_A

λ_A/(W/(m·K))	ΔT/K	q/(W/m^2)	R/((m^2·K)/W)	K/(W/(m^2·K))
0.3	26.760	58.679	0.4560	1.6500
0.4	26.756	58.725	0.4556	1.6512
0.5	26.754	58.753	0.4554	1.6519
0.6	26.753	58.771	0.4552	1.6523

When λ_A increases from 0.3 W/(m·K) to 0.6 W/(m·K), the heat transfer coefficient K of B6(20)E0 increases by only 0.139% from 1.6500 W/(m^2·K) to 1.6523 W/(m^2·K), which can be neglected. Therefore, the effect of different λ_A on the heat transfer coefficients of all tested walls can be neglected and the thermal conductivity coefficient of the adhesive λ_A is chosen to be 0.3 W/(m·K) in the following finite element analysis.

3.1.4 Comparison of Results of Numerical and Experimental Results

Based on the above modeling method, models B3(40)E0 and B5(30)E1 are established to conduct heat transfer analysis. The temperature distribution contours of models B3(40)E0 and B5(30)E1 are shown in Fig. 11. The heat flow density distribution contours of the two models in the X, Y and Z directions are shown in Fig. 12 and Fig. 13, respectively. According to Fig. 11, the temperature distributes uniformly in X and Y directions and varies in a gradient in Z direction. The temperature decreases gradually along Z direction because of thermal insulation effect of the wall. As seen from Fig. 12 and Fig. 13, the magnitude of heat flow density in X and Y direction is only 10^{-12}, which can be ignored. Therefore, the assumption of one-dimension heat transfer can be accepted when the length and width of the specimen are much larger than the thickness.

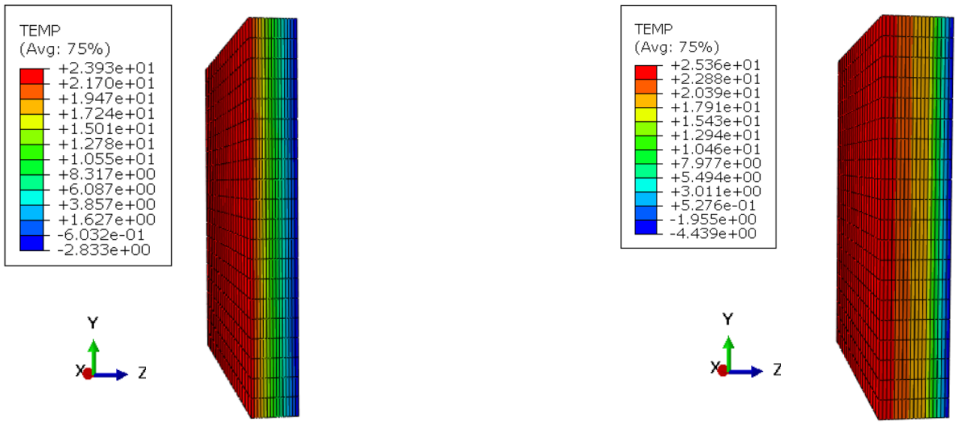

(a) B3(40)E0 (b) B5(30)E1

Figure 11: Temperature distribution contours

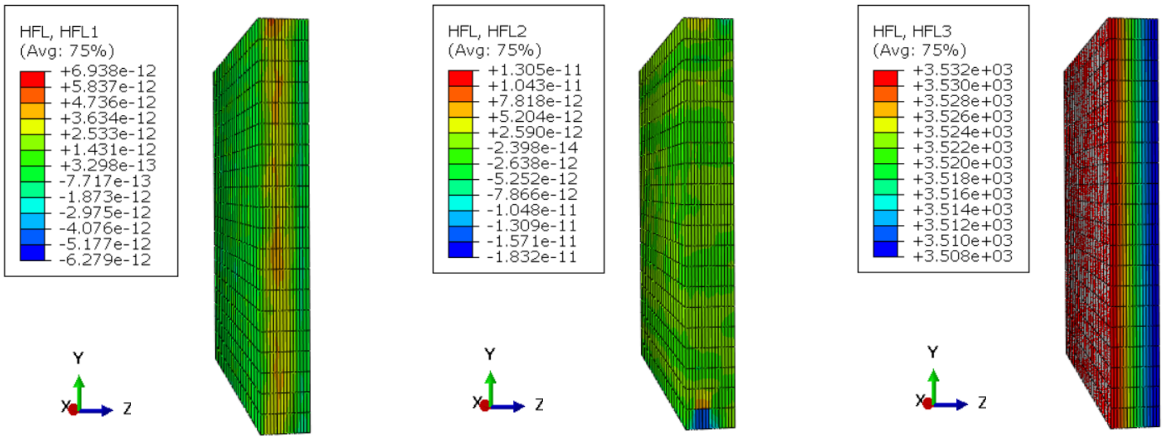

(a) X direction (b) Y direction (c) Z direction

Figure 12: Heat flow density distribution contours of the model B3(40)E0

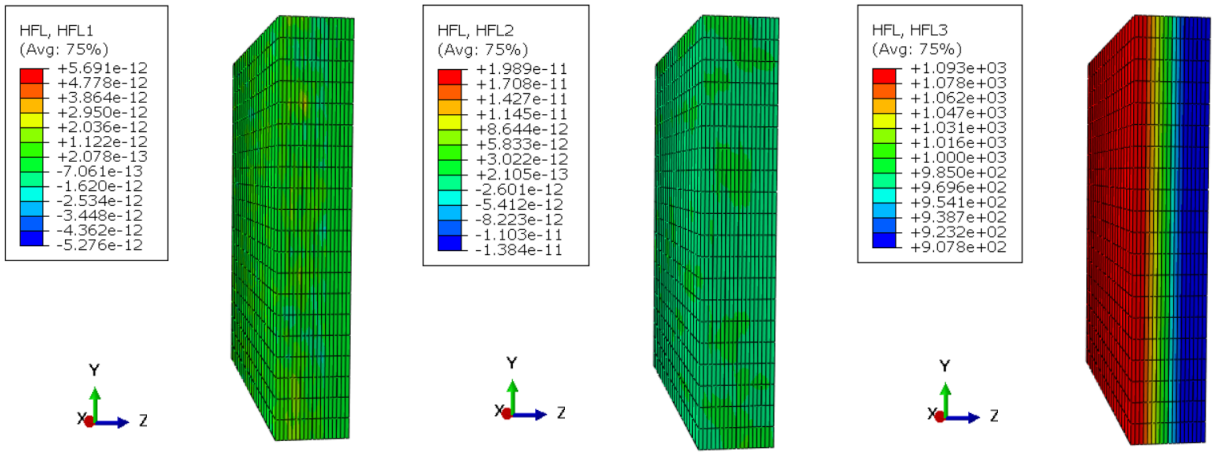

(a) X direction (b) Y direction (c) Z direction

Figure 13: Heat flow density distribution contours of the model B5(30)E1

The variation of temperatures on both sides of the wall and heat flow density inside the wall along with time is compared with experimental results, as shown in Fig. 14 and Fig. 15. Because the temperature changes along X and Y direction are very small and can be ignored, the temperatures of central points of inner and outer surface in the finite-element model are selected as comparative data. The average temperature measured by six temperature measuring points introduced in Section 2.2.2 is used as the experimental temperature. The heat flow density of central point of inner surface (hot surface) in finite element model and the average value of the heat flow densities measured by three heat flow measuring points introduced in Section 2.2.2 are taken as numerical data and experimental data, respectively.

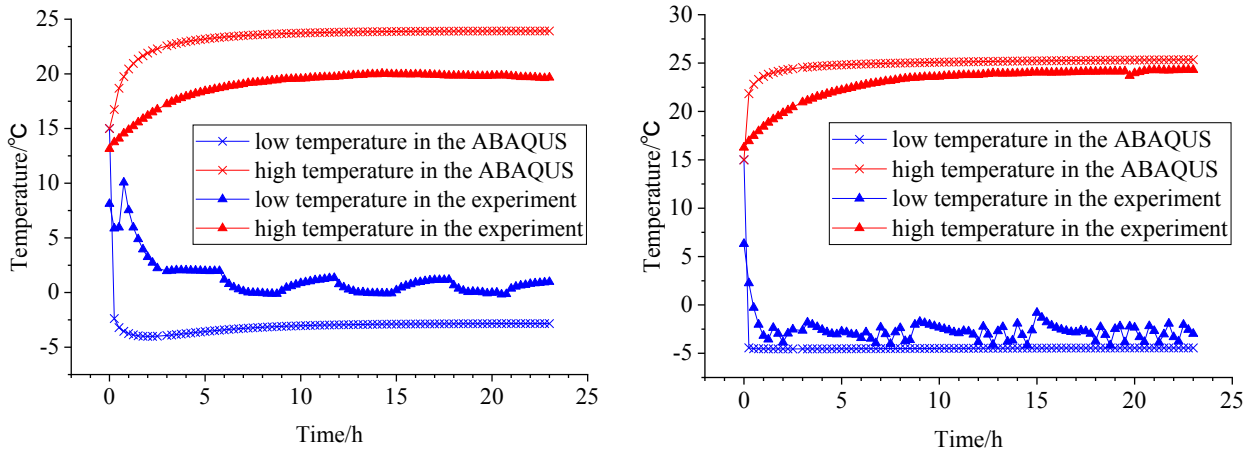

(a) B3(40)E0 (b) B5(30)E1

Figure 14: Comparison of temperature-time curves obtained from FEA and experiment

From Fig. 14, the experimental temperature cannot reach the temperature calculated by the finite element method. There are probably two reasons which can explain this phenomenon. The first reason is that there are still some voids between the specimen and specimen holder in the experiment to produce the air convection between hot box and cold box, although the polyurethane foaming agent is used to fill the voids around the specimen. The second reason is that the heat loss exists in the actual experiment, which is not taken into account in the finite element calculation.

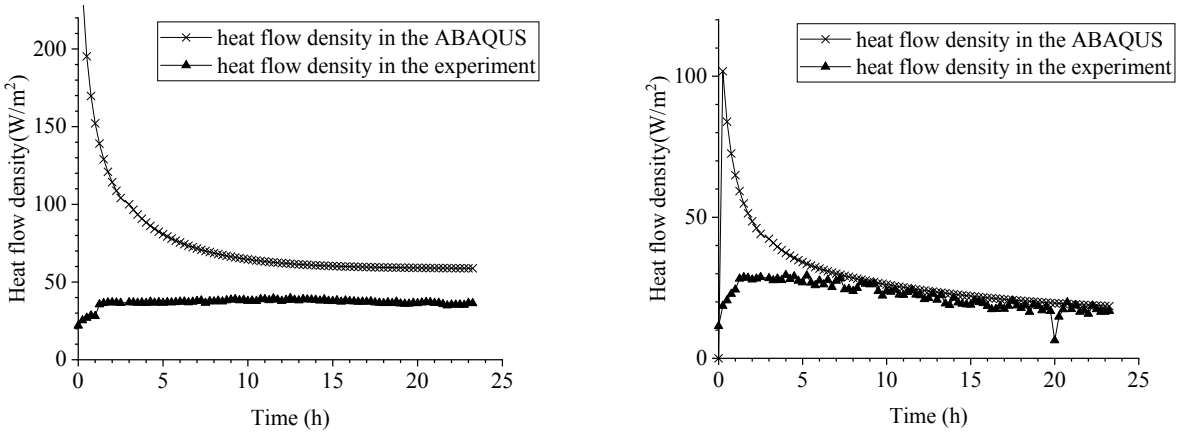

(a) B3(40)E0 (b) B5(30)E1

Figure 15: Comparison of heat flow density-time curves obtained from FEA and experiment

Fig. 15 shows that the simulation values obtained by FEA are higher than the experimental values. This may be due to the second assumption introduced in Section 3.1.1 that the interfaces between layers of the wall are fully contacted and the influence of interface thermal resistance is not considered. In fact, the simulation results are higher than the experimental results because of the voids and interface thermal resistance in the actual specimens. According to Eqs. (2) and (3) in the Section 2.2.2, the simulation value of heat transfer coefficient K_s can be calculated and compared with experiment results K_e, as listed in Tab. 9. The error between K_e and K_s of the two specimens is less than 13%, which demonstrated the accuracy of the proposed finite element model.

Table 9: Comparison of FEA and experiment results

Label	R_s/(W/(m^2·K))	K_s/(W/(m^2·K))	K_e/(W/(m^2·K))	($\|K_s$-$K_e\|$/K_e)
B3(40)E0	0.455	1.654	1.467	12.75%
B5(30)E1	1.635	0.560	0.567	1.23%

3.2 Effect of EPS Foam Plate Location on Heat Transfer Coefficient in the EPS-CLB Composite Wall

The simulation value of heat transfer coefficient calculated by ABAQUS is proved to be efficient, the numerical model can thus be used to analyze the effect of EPS foam plate location on heat transfer coefficient in the EPS-CLB composite wall. Three B4(30)E1 models with different positions of EPS foam plate have been established, namely, the EPS foam plate placed on the cold side of CLB wall, the hot side of CLB wall and in the middle of CLB wall. These three models are named as Cold, Hot and Middle, respectively. The temperature distribution contours and heat flow density distribution contours in Z direction of models were obtained, as shown in Fig. 16 and Fig. 17, respectively.

It can be seen from Fig. 16 and Fig. 17, the temperatures and heat flow densities of these three models are very close after entering into the steady state of heat transfer. According to Eqs. (2) and (3) in the Section 2.2.2, the simulation value of heat transfer coefficients of these three models can be calculated and compared, as shown in Tab. 10. As listed in Tab. 10, the heat transfer coefficients of the cases Cold and Hot are 0.56% and 2.79% higher than that of the case Middle, respectively. The effect of thermal insulation is best when EPS foam plate is placed in the middle of EPS-CLB composite wall. However, the construction quality of the sandwich insulation is difficult to be inspected and the sandwich insulation will produce thermal bridge [39]. Therefore, the EPS-CLB composite wall adopting external thermal insulation (the EPS foam plate placed on the cold side of the wall) is relatively recommended, considering both of the thermal insulation effect and construction quality.

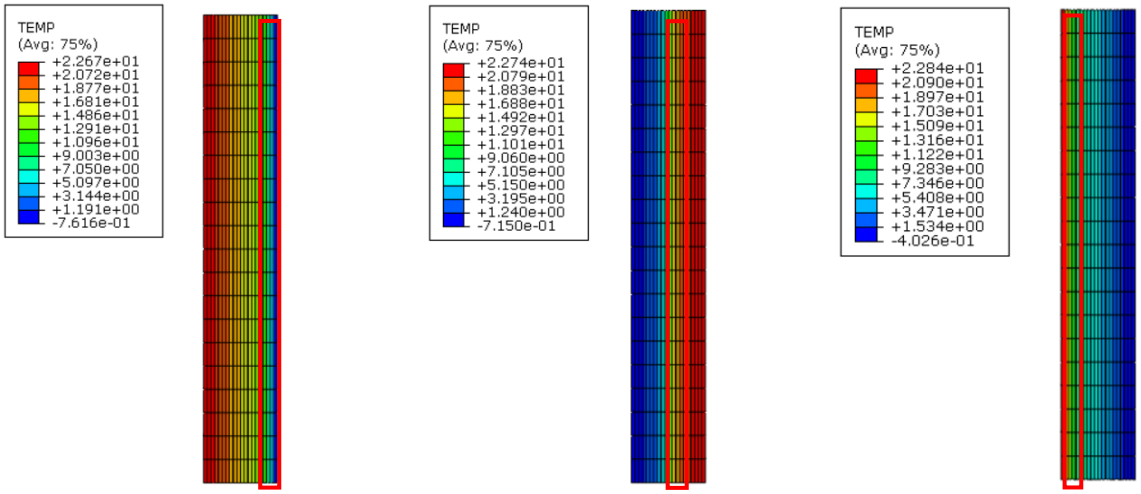

(a) EPS foam placed on the cold side

(b) EPS foam placed in the middle

(c) EPS foam placed on the hot side

Figure 16: Temperature distribution contours of EPS-CLB composite walls

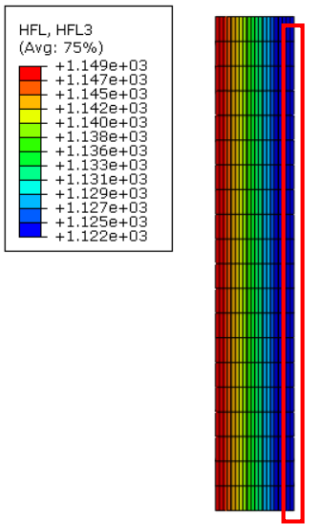

(a) EPS foam placed on the cold side

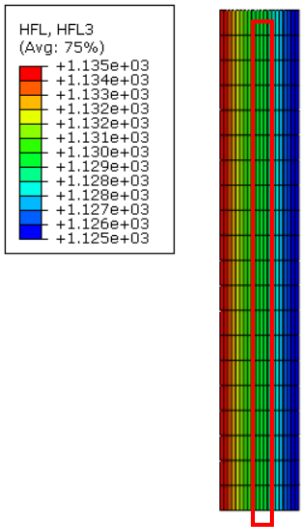

(b) EPS foam placed in the middle

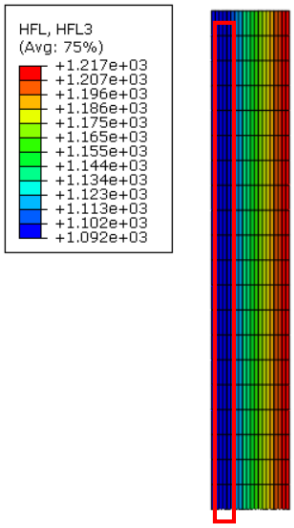

(c) EPS foam placed on the hot side

Figure 17: Heat flow density distribution contours of EPS-CLB composite walls

Table 10: Comparison of FEA results of three different models

Numerical case	Temperature difference /K	Heat flow density /(W/m^2)	Thermal resistance /((K·m^2)/W)	Heat transfer coefficient /(W/(K·m^2))
Cold	23.434	18.924	1.238	0.720
Middle	23.459	18.832	1.246	0.716
Hot	23.244	19.242	1.208	0.736

4 Conclusion

The thermal conductivity coefficients of bamboo scrimber plate and EPS foam plate are tested through guarded hot plate method. The heat transfer coefficients of CLB walls and EPS-CLB composite walls are tested through the temperature-controlled box-heat flow meter method and compared with the theoretical derivations. Furthermore, the influence of different locations of the EPS foam plate on the thermal insulation performance is analyzed by the finite element method. Based on experimental, theoretical and numerical analyses, the following conclusions can be drawn:

1. The thermal conductivity of bamboo scrimber plate λ_B is about 0.263 W/(m·K), which is far fewer than that of most existing common inorganic materials used in building, about 15% of reinforced concrete and about 50% of hollow brick and light-weight aggregate concrete. λ_B slightly increases with the increase of the average temperature on both sides of the bamboo scrimber plate. The thermal conductivity of EPS foam plate λ_E is 0.04 W/(m·K).
2. The heat transfer coefficient K of the CLB wall decreases with the increase of the thickness of the wall. The effect of configuration on K can be ignored. The heat transfer coefficient of EPS-CLB composite wall with one layer of EPS foam plate is significantly lower than that of CLB wall with no EPS foam plate. In terms of improving the thermal insulation effect, the efficiency of adopting two layers of EPS foam plates is obviously reduced when compared with the efficiency of adding one layer of EPS foam plate. The theoretical calculations of the heat transfer coefficient of composite walls are compared with the experimental values. The average error is about 15.36%, which is acceptable.

3. According to Chinese standard [28-31], most CLB walls can be used in Moderate climate (B) zone and Hot summer and Warm winter zone. However, the EPS-CLB composite walls can be used in Moderate climate (A) zone, Hot summer and cold winter zone and even Cold zone.
4. When thermal conductivity coefficient of adhesive λ_A ranges from 0.3 W/(m·K) to 0.6 W/(m·K), the influence of the change of λ_A on the heat transfer coefficients of walls can be neglected. The error between the experimental and numerical results of K is less than 12.75%, which proves the validity of finite element models. The influence caused by different locations of the EPS foam plate in EPS-CLB composite wall can be neglected.

Acknowledgment: The authors would like to acknowledge financial support from the National Natural Research and Development Fund (9Z05000049D0) and Integrated Key Precast Components and New Wood-bamboo Composite Structure (2017YFC0703502).

References

1. Yang, Q., Duan, Z. B., Wang, Z. L., He, K. H., Sun, Q. X. et al. (2008). Bamboo resources, utilization and ex-situ conservation in Xishuangbanna, South-eastern China. *Journal of Forestry Research, 19,* 79-83.
2. Xie, Q. J., Xiao, Y. (2016). Experimental study on large-span glubam roof trusses. *Journal of Building Structures, China, 37,* 47-53.
3. Sharma, B., Gatóo, A., Bock, M., Ramage, M. (2015). Engineered bamboo for structural applications. *Construction and Building Materials, 81,* 66-73.
4. Zhang, Q. S., Jiang, S. X., Tang, Y. Y. (2002). *Industrial utilization on bamboo.* Colour Max Publishers Limited, HongKong.
5. Wang, G., Jiang, Z. H., Chen, F. M., Cheng, H. T., Sun, F. B. (2014). Manufacture situation and problem analysis on large size bamboo engineering material in China. *China Forest Products Industry, 41,* 48-52.
6. Sulastiningsih, I. M., Nurwati (2009). Physical and mechanical properties of laminated bamboo board. *Journal of Tropical Forest Science, 21(3),* 246-251.
7. Li, H. T., Liu, R., Lorenzo, R., Wu, G., Wang, L. B. (2019). Eccentric compression properties of laminated bamboo columns with different slenderness ratios. *Proceedings of the Institution of Civil Engineers-Structures and Buildings, 172,* 315-326.
8. Li, H. T., Wu, G., Xiong, Z. H., Corbi, I., Corbi, O. et al. (2019). Length and orientation direction effect on static bending properties of laminated Moso bamboo. *European Journal of Wood and Wood Products,* 1-11.
9. Mahdavi, M., Clouston, P. L., Arwade, S. R. (2010). Development of laminated bamboo lumber: review of processing, performance, and economical considerations. *Journal of Materials in Civil Engineering, 23,* 1036-1042.
10. Guan, X., Yin, H. N., Liu, X. S., Wu, Q. R., Gong, M. (2018). Development of lightweight overlaid laminated bamboo lumber for structural uses. *Construction and Building Materials, 188,* 722-728.
11. Deng, J. C., Li, H. D., Wang, G., Chen, F. M., Zhang, W. F. (2015). Effect of removing extent of bamboo green on physical and mechanical properties of laminated bamboo-bundle veneer lumber (BLVL). *European Journal of Wood and Wood Products, 73,* 499-506.
12. Jin, X. B., Jiang, Z. H., Wen, X. W., Zhang, R., Qin, D. C. (2017). Flame retardant properties of laminated bamboo lumber treated with monoammonium phosphate (MAP) and boric acid/borax (SBX) compounds. *BioResources, 12,* 5071-5085.
13. Zhang, F. W., Yu, W. J. (2008). Research status and prospect of wood/bamboo reconstituted structural material. *China Forest Products Industry, 35,* 7-12.
14. Guan, M. J., Zhu, Y. X., Zhang, X. A. (2006). Comparison of bending properties of scrimber and bamboo scrimber. *Journal of Northeast Forestry University, 4.*
15. Li, H. T., Qiu, Z. Y., Wu, G., Wei, D. D., Lorenzo, R. et al. (2019). Compression behaviors of parallel bamboo strand lumber under static loading. *Journal of Renewable Materials, 7(7),* 583-600.
16. Gong, Y. C., Zhang, C. Q., Zhao, R. J., Xing, X. T., Ren, H. Q. (2016). Experimental study on tensile and compressive strength of bamboo scrimber. *BioResources, 11,* 7334-7344.

17. Kumar, A., Vlach, T., Laiblova, L., Hrouda, M., Kasal, B. et al. (2016). Engineered bamboo scrimber: Influence of density on the mechanical and water absorption properties. *Construction and Building Materials, 127,* 815-827.
18. Jin, X., Zhang, L., Li, Y., Wen, X., Qin, D. (2015). Effects of three fame retardants on combustion physical and mechanical properties of bamboo scrimber. *Journal of Northwest Forestry University, 30,* 214-218.
19. Du, C., Zhou, Z., Yu, H., Huang, Q., Yao, X. et al. (2017). Smoke-inhibiting properties and smoke characteristics of fire-retardant bamboo scrimber in burning. *Journal of Nanjing Forestry University, 41,* 163-168.
20. Chen, W. M., Li, X. G., Chen, M., Ji, Y. X., Yuan, G. M. (2014). Effect of pretreatment on bamboo strip and bamboo-wood hybrid scrimber property. *Journal of Functional Materials, 45,* 15114-15117.
21. Wu, B. L., Yu, Y. L., Qi, J. Q., Yu, W. J. (2014). Effects of bamboo bundles treated with fine fluffing and carbonized treatment on the properties of bamboo scrimber. *Journal of Nanjing Forestry University (Natural Sciences Edition), 38,* 115-120.
22. Shah, D. U., Bock, M. C. D., Mulligan, H., Ramage, M. H. (2016). Thermal conductivity of engineered bamboo composites. *Journal of Materials Science, 51,* 2991-3002.
23. Huang, Z., Sun, Y., Musso, F. (2017). Experimental study on bamboo hygrothermal properties and the impact of bamboo-based panel process. *Construction and Building Materials, 155,* 1112-1125.
24. Gao, L., Wang, Z., Chang, L. (2010). Heat and sound insulation performance of prefabricated bamboo-wood wall. *China Wood Industry, 24,* 26-28.
25. Wang, J. S., Demartino, C., Xiao, Y., Li, Y. Y. (2018). Thermal insulation performance of bamboo-and wood-based shear walls in light-frame buildings. *Energy and Buildings, 168,* 167-179.
26. *Thermal insulation-determination of steady-state thermal resistance and related properties-guarded hot plate (ISO 8302: 1991) (1991)*. International Standards Organization, Geneva.
27. *Code for thermal design of civil building (GB50176-2016) (2016)*. Beijing: China Architecture & Building Press.
28. *Design standard for energy efficiency of residential buildings in severe cold and cold zones (JGJ 26-2010) (2010)*. Beijing: China Architecture & Building Press.
29. *Design standard for energy efficiency of residential buildings in hot summer and cold winter zone (JGJ 134-2010) (2010)*. Beijing: China Architecture & Building Press.
30. *Design standard for energy efficiency of residential buildings in hot summer and warm winter zone (JGJ 75-2012) (2012)*. Beijing: China Architecture & Building Press.
31. *Standard for design of energy efficiency of residential buildings in moderate climate zone (JGJ 475-2019) (2019)*. Beijing: China Architecture & Building Press.
32. Tian, Y. L., Lu, J. M., Jiang, S. X. (2012). Study on the thermal performance of external wall of bamboo structure. *Journal of Nanjing Forestry University (Natural Sciences Edition), 36,* 96-100.
33. *Thermal insulation-determination of steady state thermal transmission properties-calibrated and guarded hot box (ISO 8990: 1994) (1994)*. International Organization for Standardization: Geneva, Switzerland.
34. *Standard for energy efficiency test of residential buildings (JGJ/T 132-2009) (2009)*. Beijing China, Architecture & Building Press.
35. *Building components and building elements-thermal resistance and thermal transmittance-calculation method (ISO 6949: 2007) (2007)*. European Committee for Standardisation.
36. Hua, Z. L., Ban, H. (2017). A new measurement approach for interface thermal resistance using frequency-scan photothermal reflectance technique. *International Journal of Thermal Sciences, 117,* 59-67.
37. Xiang, J. H. (2016). *Experimental research on properties on parallel strand bamboo at high temperature.* Southeast University, China.
38. Yang, S. M., Tao, W. Q. (2006). *Heat transfer*. Beijing Higher Education Press.
39. Chang, S. J., Wi, S., Kim, S. (2019). Thermal bridging analysis of connections in cross-laminated timber buildings based on ISO 10211. *Construction and Building Materials, 213,* 709-722.